Available online at www.sciencedirect.com
ScienceDirect
Journal of Power Sources 179 (2008) 808–818
JOURNAL OF POWER SOURCES
www.elsevier.com/locate/jpowsour

Studies of the pulse charge of lead-acid batteries for PV applications Part III. Electrolyte concentration effects on the electrochemical performance of the positive plate

A. Kirchev *, A. Delaille, F. Karoui, M. Perrin, E. Lemaire, F. Mattera

Laboratoire des Systèmes Solaires, Institut National de l'Energie Solaire, Commissariat de l'Energie Atomique, 50 avenue du Lac Léman, 73377 Le Bourget du Lac, France

Received 28 September 2007; received in revised form 9 November 2007; accepted 1 December 2007
Available online 15 December 2007

Abstract

In the third part of this work the effects of the sulphuric acid concentration on the positive plate discharge capacity, impedance and oxygen overvoltage are discussed. It has been found that the full discharge capacity of the positive plate is available down to electrolyte concentrations of 3 mol l^{-1} (s.g. 1.18 g ml^{-1}). At further acid dilution, capacity of the positive plate declines, keeping the utilization of the sulphuric acid about 50%. Decreasing the acid concentration, the oxygen overvoltage decreases with a factor of 12–18 mV M^{-1}, excluding the effect of the equilibrium potential of the oxygen electrode as a function of pH. The capacitance of the electrical double layer decrease linearly with the dilution of the sulphuric acid suggesting strong adsorption effects. This suggestion has been confirmed from the measurements of potential of the zero charge of the positive plate, which increases from 1.11 to 1.34 V vs. Ag/Ag_2SO_4 in the region 1.11–4.60 M H_2SO_4. From the measurement of the time constant of the electronic transfer through the gel part of the lead dioxide (T_{gel}) as a function of the acid concentration and the applied potential, a change in the mechanism of the lead dioxide hydration has been estimated—below 1 M H_2SO_4 T_{gel} increases sharply, showing sharp increases of the extent of the hydration. The dilution of the electrolyte increases substantially the value of average double layer current in the beginning of the charge. During the pulse overcharge at the employed frequency of 1 Hz, the average double layer current is equal to the pulse amplitude, suggesting that the maximal efficiency of the pulse charge is reached.

Keywords: Lead acid; Pulse charge; Electrochemical impedance spectroscopy (EIS); Electrochemical double layer (EDL); Positive plate; Oxygen evolution

1. Introduction

The electrolyte of the lead-acid battery is frequently denoted as the third active material due to its participation in the electrochemical reactions of charge/discharge taking place on both plates:

$$PbO_2 + HSO_4^- + 3H^+ + 2e^- = PbSO_4 + 2H_2O \quad (1a)$$

$$Pb + HSO_4^- = PbSO_4 + H^+ + 2e^- \quad (1b)$$

Thus during the discharge, the electrolyte concentration decreases and *vice versa*. However taking into account reaction (1a) it is obvious that the local variation in the acid concentration will have higher amplitude in the pores of the positive plate, due to the formation/depletion of water molecules there.

One of the most suitable types of batteries for PV applications, considering the cost-performance ratio, are the VRLA batteries with AGM separator and pasted positive plates. This conclusion is due to the improved cycle life (result of the applied compression), the maintenance free operation (result of the internal recombination of the oxygen), almost complete absence of stratification (result of the immobilization of the electrolyte in the AGM separator) as well as low internal resistance allowing high charge and discharge rates [1]. Together with the advantages of the VRLA batteries, there is one critical point which can change dramatically their performance. This critical point is connected with the limited volume of electrolyte, respectively, the limited quantity of sulphuric acid molecules. While the volume of the electrolyte in the VRLA cell can be only determined by the thickness of the AGM separator, the quantity of

* Corresponding author. Tel.: +33 4 79 44 45 49; fax: +33 4 79 68 80 49.
E-mail address: angel.kirchev@cea.fr (A. Kirchev).

0378-7753/$ – see front matter © 2007 Elsevier B.V. All rights reserved.
doi:10.1016/j.jpowsour.2007.12.015

sulphuric acid molecules can be tuned also by the electrolyte concentration. To the moment, a common approach is the use of thinner AGM separator, which slightly reduces the cost of the battery, and more concentrated electrolyte (with specific gravity 1.30–1.33 g ml^{-1}) in order to achieve 100% DOD in deep cycling conditions. The drawbacks of such choice of VRLA cell design are several:

- Hard sulphation of the positive and the negative plates, which is a result of several phenomena—operation of the oxygen cycle causing incomplete charge of the negative plates, decreased $PbSO_4$ solubility due to the higher electrolyte concentration, and long-term operation in partial state of charge (PSoC) typical for all lead-acid batteries in the solar systems [2].
- Thermal runaway due to decreased heat capacity of the cell [3,4].
- Passivation and accelerated degradation of the positive active material [5].

Thus, the understanding of the mechanisms by which the sulphuric acid concentration affects the processes during the operation of the positive plate acquires the present importance. In this connection, here the term "electrochemical performance" has few sides, which will be discussed in this work, considering only the positive plate: discharge capacity, pulse charge behaviour, oxygen evolution and electrochemical impedance.

2. Experimental

The experiments were carried out in three-electrode electrochemical cells consisting of:

- *Working electrode*. Dry-charged flat positive plate with 3 mm thickness, 3 Ah nominal capacity at 50% PAM utilization, produced by CEAC-EXIDE (France), with grid composition Pb–2.8% Sb. The plates where cut from bigger 40 Ah plates. The presence of Sb in the grid alloy ensures the absence of passivation phenomena like Sb-free effects, PCL1, PCL2, etc. Thus, it is sure that the essence of the studied phenomena will be focused in the volume of the positive active mass.
- *Counter electrode*. Two dry-charged CEAC-EXIDE (France) negative plates, with nominal capacity 3 Ah each and thickness 3 mm. The plates where also cut from bigger 40 Ah plates.
- *Reference electrode*. Ag/Ag_2SO_4 (filled with H_2SO_4, s.g. 1.28 g ml^{-1}), +38 mV vs. Hg/Hg_2SO_4 in the same solution [6,7].

The initial 10 cycles were carried out in H_2SO_4 electrolyte with s.g. 1.28 g ml^{-1}. The initial quantity of the electrolyte was measured as a weight difference between the dry-charged cell, and the cell after its filling with electrolyte. The initial volume of electrolyte was 92 ± 0.5 ml.

After 30 min of soaking in the electrolyte, the cells were subjected to a 20 h charge-up at $I = 0.1$ A in order to oxidize the residual quantities of $PbSO_4$ unconverted into PbO_2 or Pb during the formation. After this conditioning of the cells, following cycling regime was applied:

(1) Discharge: $I = -0.6$ A down to $U_{cell} = 1.75$ V.
(2) Open circuit stay: 30 min.
(3) Constant current charge: $I = 0.6$ A up to $U_{cell} = 2.5$ V.
(4) Constant voltage charge: $U_{cell} = 2.5$ V until reaching 120% of recharge.
(5) Open circuit stay: 30 min.

This group of experiments was carried out with a potentiostat/galvanostat ARBIN Instruments.

Such conditioned, two identical cells were subjected to two different series of experiments, which will be denoted as "cycling series" and "overcharge series". Both series were carried out on a potentiostat/galvanostat SOLARTRON 1470 connected with a Frequency Response Analyser SOLARTRON 1250. All impedance measurements were performed with AC potential amplitude 5 mV, and spectral density of 20 points per decade in the frequency range 50 kHz to 50 mHz. The impedance results were fitted with Z-View2 software.

During the "cycling series", the cell was subjected to two charge/discharge cycles in each studied acid concentration. Prior to the cycles, part of the electrolyte in the cell was replaced with water in order to reach the desired acid concentration. The weight of the cell was registered. After this operation, the cell was subjected to 5 h open circuit stay and 20 h overcharge with 0.035 A. Thus the positive plate was both fully charged and the electrolyte became equally distributed everywhere in the cell. The discharge during the first cycle was continuous, with a current of 0.5 A until potential of the positive plate dropped to +0.7 V (vs. reference electrode). After 2 h open circuit stay the impedance spectrum of the positive plate was measured. The second discharge was interrupted at 50 ± 3% SoC (state of charge) by 2 h open circuit stay and next impedance spectrum measurement. The recharge was carried out with pulse current with the following profile: $t_{ON} = 0.5$ s and $I = 0.5$ A; $t_{OFF} = 0.5$ s and $I = 0$ A, which corresponds to frequency $f = 1$ Hz, duty cycle ratio $r = 0.5$ and pulse current amplitude $I_a = 0.5$ A. Each recharge was interrupted at about 50% SoC by 2 h open circuit period in order to measure the impedance spectrum of the positive plate at PSoC (partial state of charge) during the charge. The pulse charge was performed with factor of charge (FC, the ratio between the charged and discharged number of Ampere hours) of 105% in order to avoid intensive gassing. In the end of the second cycle the cell was subjected to 3 h potentiostatic charge at 1.3 V (vs. Ag/Ag_2SO_4) in order to reach complete charge state. In the end of this period, after 2 h open circuit stay, the impedance spectrum of the positive plate was measured again. Finally the acid density was measured with accuracy ± 0.001 g ml^{-1}, and the water loss was determined by the weight loss. In order to simplify the discussion, the average acid concentration was taken into account, considering the measured final value of the electrolyte concentration, and the calculated initial value of the electrolyte concentration, using weight loss data considered as a water loss. The acid concentration values, as well as the diffusion potential data, are listed in Table 1 for both series of experimental data.

Table 1
Values of the transport numbers, activity coefficients and diffusion potential of the sulphuric acid species H^+ and HSO_4^- for the employed electrolyte concentrations

H_2SO_4 molarity (mol l^{-1})	Specific gravity (g ml^{-1})	H_2SO_4 molality (mol kg^{-1})	Transport number	Activity coefficient	Diffusion potential (V)
"Cycling" series					
4.93	1.283	3.84	0.76	2.33	0.0000
4.17	1.243	3.35	0.77	1.91	−0.0047
3.09	1.183	2.61	0.78	1.42	−0.0128
2.04	1.123	1.82	0.80	1.06	−0.0232
1.04	1.063	0.98	0.81	0.84	−0.0377
0.53	1.032	0.51	0.81	0.77	−0.0505
0.26	1.0155	0.26	0.82	0.74	−0.0626
"Overcharge" series					
4.60	1.266	3.63	0.77	2.14	−0.0019
4.10	1.237	3.31	0.77	1.87	−0.0051
3.12	1.185	2.63	0.78	1.43	−0.0126
2.14	1.128	1.90	0.79	1.09	−0.0221
1.11	1.067	1.04	0.81	0.85	−0.0364
0.57	1.035	0.55	0.81	0.77	−0.0491
0.27	1.016	0.27	0.82	0.74	−0.0622

During the "overcharge series" the cell was subjected either to overcharge polarization or to open circuit stay. Three overcharge modes were employed: galvanostatic, potentiostatic and pulse mode. The galvanostatic and the pulse mode were the same as those used in the fist part of this work: $f = 1$ Hz and $r = 0.5$, using current amplitudes between 1 mA and 4 A. The potentiostatic mode was applied from few millivolts above the open circuit potential up to the current limit of the potentiostat (4 A) with a step of 25 mV. Each value of the potential was kept until a steady state current was reached. In the end of this period, the impedance spectrum was measured keeping the same potential.

The adjustment of the acid concentration has been done by the above-mentioned approach.

Using the same wire configuration, the obtained impedance spectra were subjected to inductance error correction procedure [8].

3. Results and discussion

3.1. Influence of the electrolyte concentration on the charge/discharge performance of the positive plate

The most important characteristic of the positive plate is its discharge capacity. The discharge curves at 6-h rate are shown in Fig. 1a. It is evident that the maximum capacity of the positive plate is available down to about 3.2 M H_2SO_4 (s.g. 1.18 g ml^{-1}).

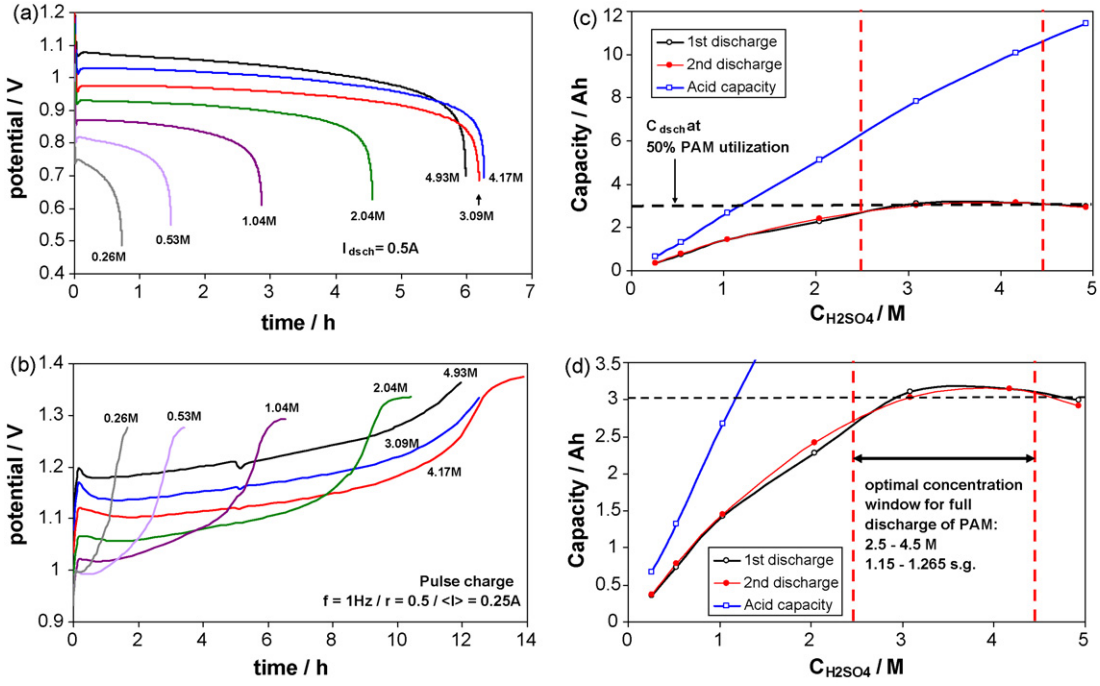

Fig. 1. Discharge (a) and charge (b) positive plate potential transients in electrolyte with different concentration. (c and d) Dependence of the discharge capacity of the positive plate and the electrochemical equivalent of the electrolyte (denoted as "acid capacity") on the sulphuric acid concentration.

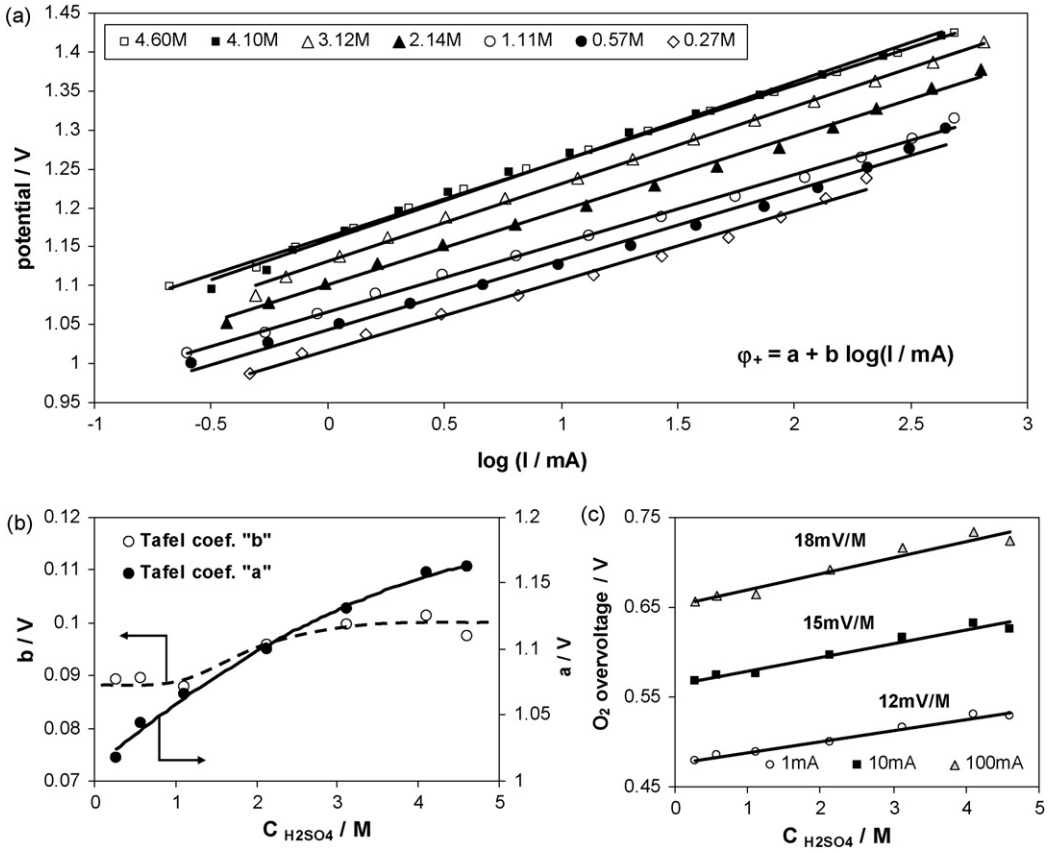

Fig. 2. (a) Tafel plots for the process of oxygen evolution in H_2SO_4 with different concentration. (b) Dependence of the Tafel coefficients on the H_2SO_4 concentration. (c) Dependence of the oxygen overvoltage on H_2SO_4 concentration.

Below this value, the available capacity of the positive plate decreases rapidly. The average value of the discharge potential also decreases with the decrease of the acid concentration, which is expected considering the thermodynamics of the positive plate and the increased electrolyte resistance causing the ohmic drop in the electrolyte. The equilibrium potential of the $PbSO_4/PbO_2$ electrode decreases both with the increase of the pH and with the decrease of the activity of the SO_4^{2-} and HSO_4^- species [6,7]:

$$E_{PbSO_4/PbO_2} = 0.921 - 0.059\,\mathrm{pH} + 0.059\,\lg a_{HSO_4^-} \quad (\text{vs. } Ag/Ag_2SO_4) \qquad (2)$$

The same electrochemical behaviour can be seen during the recharge of the positive plate (Fig. 1b). Here the charge transients were built using the values of the positive plate potential (φ_+) in the end of the "ON" period of the pulse. Considering the fact that the initial state for each acid concentration value is with charged plate, it is obvious that the discharge process is the one, which limits the performance of the positive plate. This hypothesis was confirmed by the comparison between the discharge capacity values obtained during the first and the second discharge presented in Fig. 1c and d—they are almost identical. Furthermore, since the second discharge is interrupted by 2 h open circuit stay and next 46 min of EIS measurement at the open circuit potential, it is obvious that the concentration gradient between the bulk electrolyte and the PAM pores is not the main reason for the decease of the capacity when the acid concentration is below 3 M. The Ah-equivalent of the sulphuric acid in the cell was also calculated and presented in Fig. 1c and d (the "acid capacity" curve). In the point corresponding to the beginning of the capacity decline (~2 M H_2SO_4, s.g. 1.125 g ml^{-1}) the Ah-excess of electrolyte is still substantial compared to the nominal capacity of the plate, but the discharge process is already limited by the electrolyte. At further decrease of the acid concentration the ratio between the discharge capacity and the "acid capacity" remains about 50%. Thus the minimal acid concentration at which the complete capacity of PAM is available at huge volume excess of electrolyte will correspond to about 2.5 M (s.g. 1.15 g ml^{-1}).

The results differs form the recent results of Pavlov et al. [5] according to which the battery capacity begins to drop substantially at acid densities below 1.21 g ml^{-1} (3.572 M). The observed difference is due to the huge volume excess of electrolyte in our studies, compared with the regular VRLAB design used by Pavlov et al., where the volume of the electrolyte is rather limited by the thickness of the AGM separator.

3.2. *Influence of the electrolyte concentration on the process of oxygen evolution*

While the oxygen evolution process is responsible for the water loss in the flooded batteries (together with the hydrogen

evolution on the negative plate), in the VRLA batteries this process determines almost entirely the rate and the efficiency of the oxygen cycle [9]. The Tafel plots obtained during the potentiostatic polarization in the different electrolytes are shown in Fig. 2a. It is clear that the dilution of the electrolyte decreases substantially the oxygen overvoltage. However the slope of all lines remains almost the same for all acid concentrations, which supposes no change in the mechanism of the oxygen evolution process. The obtained values of the Tafel coefficients "*a*" and "*b*" are plotted vs. the acid molarity in Fig. 2b. The Tafel slope "*b*" increases step-like from 90 to 100 mV between 1 and 2 M H_2SO_4. The result is in very good agreement with the data reported by Dimitrov [10], for model PbO_2 electrodes obtained by oxidation of pure lead electrode. The evolution of the "*a*" parameter is also close to the above-mentioned publication—for 10 times of acid dilution the residual "*a*" rises with about 110 mV, and the value of ~100 mV is obtained by Dimitrov. The obtained Tafel plots for the oxygen evolution at different electrolyte concentrations seem quite similar to the Tafel plots for the oxygen evolution at different temperatures [11]. Therefore it can be interesting to introduce here a concentration coefficient of the oxygen overvoltage in analogy with the corresponding temperature coefficient. The oxygen overvoltage was calculated as the difference between the potential of the electrode measured under some applied current and the equilibrium potential of the oxygen overvoltage reaction according to the following Nernst equation:

$$E_{H_2O/O_2} = 0.581 - 0.029\,\mathrm{pH} + 0.029a_{HSO_4^-}$$
$$(\text{vs. } Ag/Ag_2SO_4 \text{ reference electrode}) \quad (3)$$

Since the potential is measured vs. Ag/Ag_2SO_4 reference electrode the term "$0.029a_{HSO_4^-}$" accounts the influence of the concentration of the HSO_4^- ions in the system. The dependence of the oxygen overvoltage on the acid concentration for several overcharge currents is plotted in Fig. 3c. The values of the concentration coefficient of the oxygen overvoltage rise from 12 mV M^{-1} for small overcharge currents to 18 mV M^{-1} for current equal to 100 mA (or 30 h charge rate). These values can be used for corrections in the floating and charge regimes in order to prevent the development of negative phenomena like accelerated water loss, positive grid corrosion and thermal runaway caused by the decreased oxygen overvoltage in cells with more diluted acids.

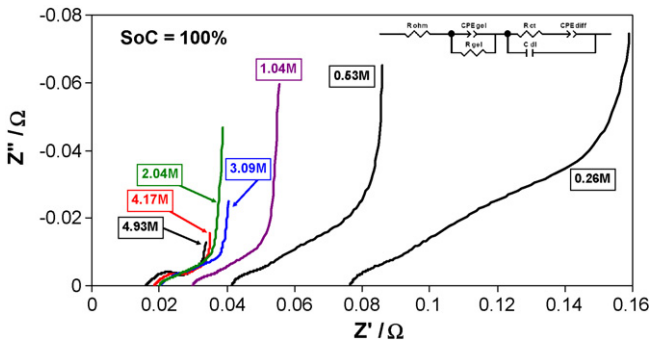

Fig. 3. Evolution of the positive plate impedance spectrum with the acid concentration at SOC = 100% during the "cycling" series in the frequency domain 50 kHz to 50 mHz.

3.3. Influence of the electrolyte concentration on the impedance of the positive plate during the cycling series

The strong variation of the positive plate discharge capacity at the different electrolyte concentrations rises the question about the point of view, from which an adequate comparison of the impedance data can be done. The completely charged state offers the best opportunities of such comparison.

The impedance spectra after both cycles and the float recharge are presented in Fig. 3. The employed fitting model (also shown in Fig. 3) was discussed in details in Part II of this work. In brief, R_{ohm} stands for the resistance of the electrolyte and the conductive parts of the electrode (cables, current collectors, active material which does not participate in the electrochemical reaction, etc.), R_{gel} stands for the resistance of the gel part of the lead dioxide, CPE_{gel} accounts both the dielectrical properties and the anisotropy of this gel part, R_{ct} is the charge transfer resistance, C_{dl} is the electrochemical double layer (EDL) capacitance and CPE_{diff} accounts the diffusion of the electrolyte in the pores of the positive plate. CPE_{gel} was converted into capacitance [12,13] and the time constant T_{gel} was calculated in order to characterize the rate of the electron transport through the gel part of the lead dioxide. The results from the equivalent circuit fitting are summarized in Fig. 4. The ohmic and the charge transfer resistance of the positive plate have very similar character—in the concentration region between 5 and 2 M H_2SO_4 their values do not change substantially. At further dilution of the electrolyte, both resistances increase sharply. This result correlates well with the data in Fig. 1d—at the same point (~2 M H_2SO_4) the discharge capacity starts to decrease rapidly. In order to understand the data shown in Fig. 4a, the dependence of the specific resistance of the acid on its concentration [14] was compared with the dependence of the ohmic resistance of the cell. Both curves have very similar evolution, but the most interesting feature is that both resistance parameters (R_{ohm} and ρ_{acid}) are almost constant between 2 and 5 M H_2SO_4. In part II of this work we showed that R_{ohm} depends substantially on state of charge and state of health [15]. In the same time, the variation of the electrolyte concentration with SoC was between 4.5 M (SoC = 100%) and 2.95 M (SoC = 0%). Thus we can conclude that the changes in the ohmic resistance R_{ohm} of the positive plate for different SoC values reported in the second part of this work [15] are not result from the variation in the acid concentration during the charge and the discharge. So R_{ohm} should reflect the changes in the conductivity of the crystalline part of the PbO_2.

While R_{ohm} is a "volume" characteristic, R_{ct} is purely a "surface" one—Fig. 4b shows that at 2 M H_2SO_4 the structure of EDL passes a critical threshold, which impedes the discharge process and limits the plate capacity.

Fig. 4c shows that the capacitance of EDL increases with the increase of the acid concentration almost linearly. This effect can be associated with the chemisorption of the sulphuric acid species (H_2SO_4, HSO_4^- and SO_4^{2-}) on the surface of the lead dioxide [16].

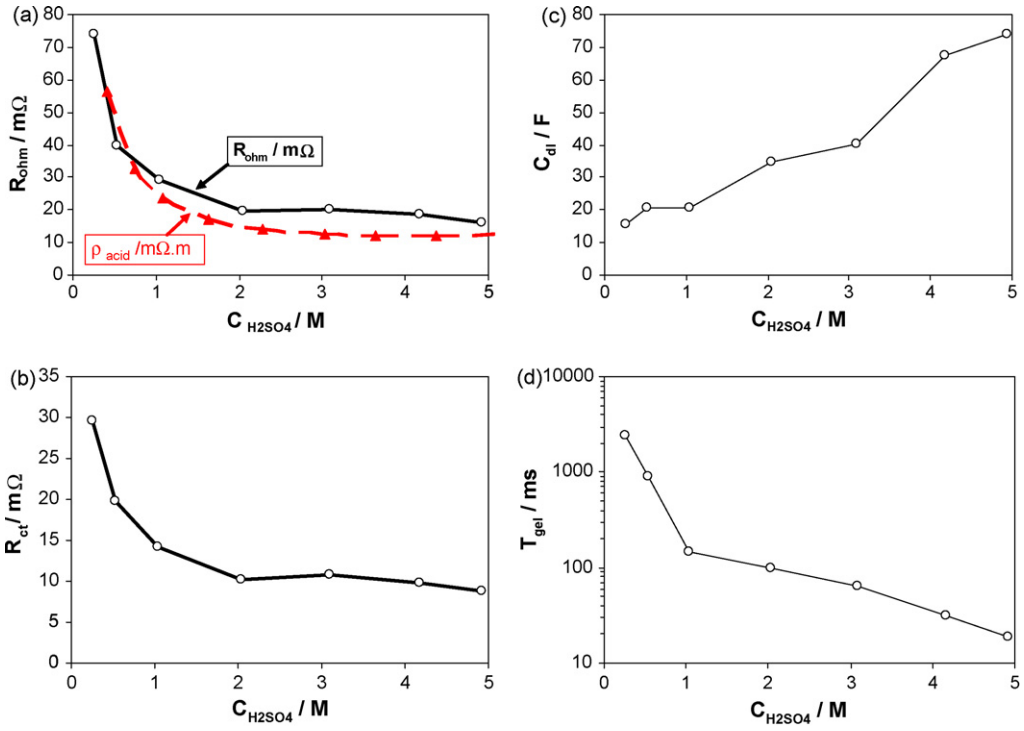

Fig. 4. Dependence of ohmic resistance (a), charge transfer resistance (b), EDL capacitance (c) and time constant of the gel part of the lead dioxide (d) on the H_2SO_4 concentration.

An interesting relation can be seen in Fig. 4d between the acid concentration and the properties of the gel part of the lead dioxide: decreasing the acid concentration, the time constant T_{gel} increases exponentially, featuring a change in the slope at about 1 M H_2SO_4. This result is not unexpected—the dilution of the acid increases the chemical potential of the water in the electrolyte and forces the hydration of the crystalline lead dioxide. The increased slope of the Log(T_{gel}) vs. $C_{H_2SO_4}$ at concentration 1 M shows that the decreased discharge capacity of the positive plate in diluted acids is also due to too high extent of hydration, which depresses the electronic conductivity of the gel part of the lead dioxide.

3.4. Influence of the acid concentration on the processes during the open circuit stay of the positive plate

In the first part of this work [17], a special attention was paid to the analysis of the open circuit decay transients at different SoC values, applying an approach proposed by Conway in the research of super-capacitor electrodes [18,19]. This analysis is an important step in the studies of the pulse charge mechanism, because it gives information about what happens during the "OFF" periods of the pulse profile. For short open circuit periods (up to about 100 min) the charge or the discharge of the EDL is coupled with some charge transfer processes—either oxygen evolution or $PbSO_4$ oxidation if the positive plate was subjected previously to a charge or reduction of PbO_2 if the previous stage has been a discharge. Regardless of the case, the relation between the potential and its rate ($d\varphi_+/dt$) is given by the equation:

$$I_{DL} = \pm C_{DL}\left(\frac{d\varphi_+}{dt}\right) = I_0 \exp\left(\frac{n\alpha F\varphi_+}{RT}\right) \quad (4)$$

where the term (RT/2.303$n\alpha F$) is equivalent to the Tafel slope "b", α is the charge transfer coefficient, n is the number of charges participating in the reaction, T is the temperature, R and F are the molar and the Faradic constants. I_0 is the exchange current of the electrochemical reaction, and C_{dl} is the value of EDL capacitance. The open circuit decay transients measured after 50% recharge are presented in Fig. 5a. At this SoC, the polarization of the positive plate is rather low and the self-discharge process is lumped only with the process of $PbSO_4$ oxidation. The derivative $d\varphi_+/dt$ was calculated in order to built the plots of Log($d\varphi_+/dt$) vs. φ_+. In the acid concentration range from 3 to 5 M H_2SO_4 all points follow a straight line, according to Eq. (4). The obtained "b" coefficient characterizing the mechanism of the charge transfer process is about 20 mV. These data are identical with the ones reported in part one of this work. In more diluted acids the deviation from Eq. (4) is obvious. The reason for this deviation is due to the fact that Eq. (4) is valid when $n\alpha F\varphi_+ \gg RT$, i.e. when the electrode potential φ_+ is substantially higher than its equilibrium value. Thus when the acid is more diluted, there will be an additional exponent term "$-I_0 \exp(-nF(\alpha-1)\varphi_+/RT)$" in accordance with the Volmer's equation. The corresponding values of the equilibrium potential of the $PbSO_4/PbO_2$ electrode are given in Fig. 5b as straight vertical lines. It is evident that in the end of the open circuit period the values of φ_+ measured in more diluted electrolyte are closer

to the corresponding equilibrium values. In the calculation of the "*b*" coefficient, in the acid concentration range 0.25–2 M H_2SO_4, only the initial straight-line section has been taken into account. The coefficient "*b*" rises from 38 mV in 2.08 M H_2SO_4 to 50–60 mV in more diluted electrolytes, indicating difficulties in the charge transfer process. The result is in fair agreement with the above-mentioned impedance results showing increased charge transfer resistance in diluted electrolytes.

The general conclusion which can be drawn from these results is that in the acid concentration range 2.5–4.5 M H_2SO_4 the rate of the EDL self-discharge process remains relatively high, which ensures the high efficiency of the pulse charge. In the same region the full capacity of the positive plate is available, when the volume of the electrolyte ensures at least 50% utilization of the H_2SO_4.

3.5. Impedance of the positive plate under potentiostatic overcharge polarization

An important circumstance for a successful application of the equivalent circuit approach in the fitting of electrochemical impedance data is setting of the studied system to a steady state, i.e. both the current flowing through the cell and the potential of the electrode should be constant during the time of the whole frequency scan. In partial SoC, this condition can be achieved usually only after some period of open circuit stay. But in completely charged state, the only process which takes place during the polarization of the positive plate is the oxygen evolution (if the grid corrosion is neglected). Under such condition, it is quite easy to achieve a steady state of the electrode at different values of the electrode potential, and thus to perform reliable impedance measurements.

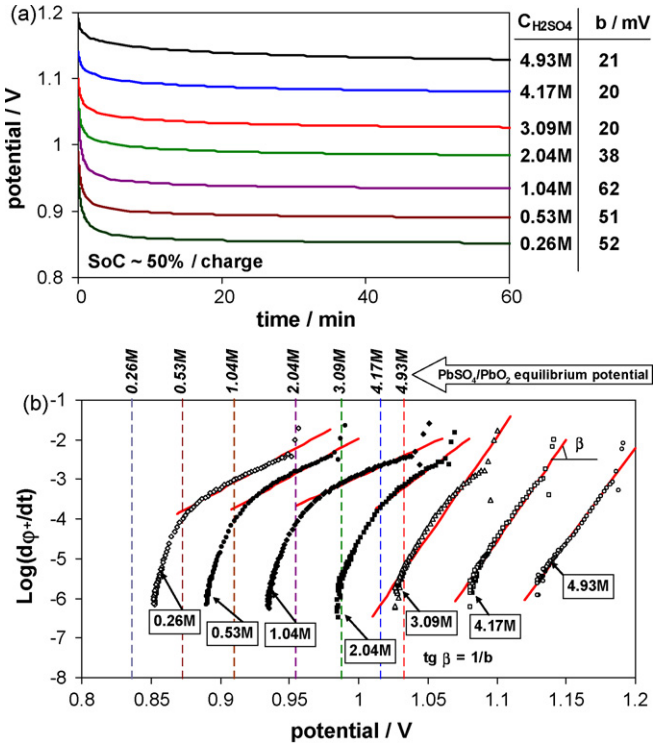

Fig. 5. (a) Open circuit decay transients at 50% SoC at different electrolyte concentrations and (b) EDL self-discharge plots.

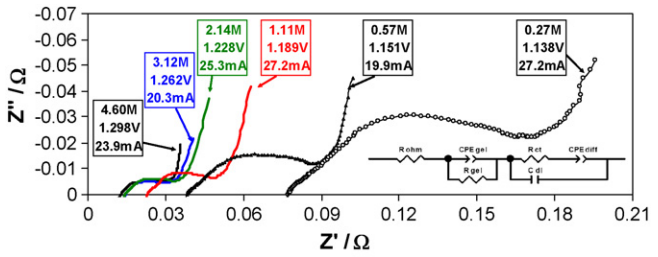

Fig. 6. Evolution of the positive plate impedance spectrum with the acid concentration at SoC = 100% during the "overcharge" series in the current range 20–30 mA, between 50 kHz and 50 mHz.

Examples of the obtained impedance spectra under potentiostatic polarization are shown in Fig. 6 for the overcharge current domain 20–30 mA (~100 h charge rate). In general the shape of the Nyquist plots does not change substantially while increasing the applied potential. For polarizations of 100–150 mV above the open circuit potential, the spectra are almost identical to the ones measured at open circuit. For this reason the same equivalent circuit model was used to fit the impedance data obtained at different potentials. The fitting gave adequate results up to values of the positive plate potential corresponding to about 0.3 A value of the overcharge current. Above this value of the current, both in the impedance spectra and in the potentiostatic current transients, the noise is substantial, which is due to the intensive gassing. In the current range 0.03–0.3 A the level of the noise was substantially lower and the fitting was successful. The evolution of the double layer capacitance and overcharge current, the charge transfer resistance and the time constant of the gel part of the lead dioxide with the positive plate potential and the acid concentration is presented in Fig. 7a–c.

3.5.1. Structure of the EDL during the overcharge

During the overcharge, the EDL is built by non-solvated H^+ ions situated on the inner Helmholtz plane produced by the decomposition of the water to oxygen and chemisorbed SO_4^{2-} and HSO_4^- ions and H_2SO_4 molecules. The evolution of the C_{dl} vs. φ_+ is very similar in the range 2–5 M H_2SO_4: while the current of the oxygen evolution is small (φ_+ is in the passive potential zone of the oxygen evolution [11]) C_{dl} is rather constant. At further polarization, C_{dl} passes a minimum which indicates the potential (point) of the zero charge (PZC) of the electrode and next a maximum which can be related to some adsorption/desorption process [20]. The potential of the zero charge reflects the following state of the lead dioxide surface:

$$\Gamma(H^+) - \Gamma(HSO_4^-) - 2\Gamma(SO_4^{2-}) = 0 \quad (5)$$

where $(\pm n)\Gamma(i)$ is the adsorption (in mol cm^{-2}) of the ion "i" with a charge $(\pm n)$. At potentials lower than PZC, there is an excess of anions in the EDL, and *vice versa*. Hence it is clear that the structure of the EDL during the overcharge is determined in greatest extent by the process of the oxygen evolution, which

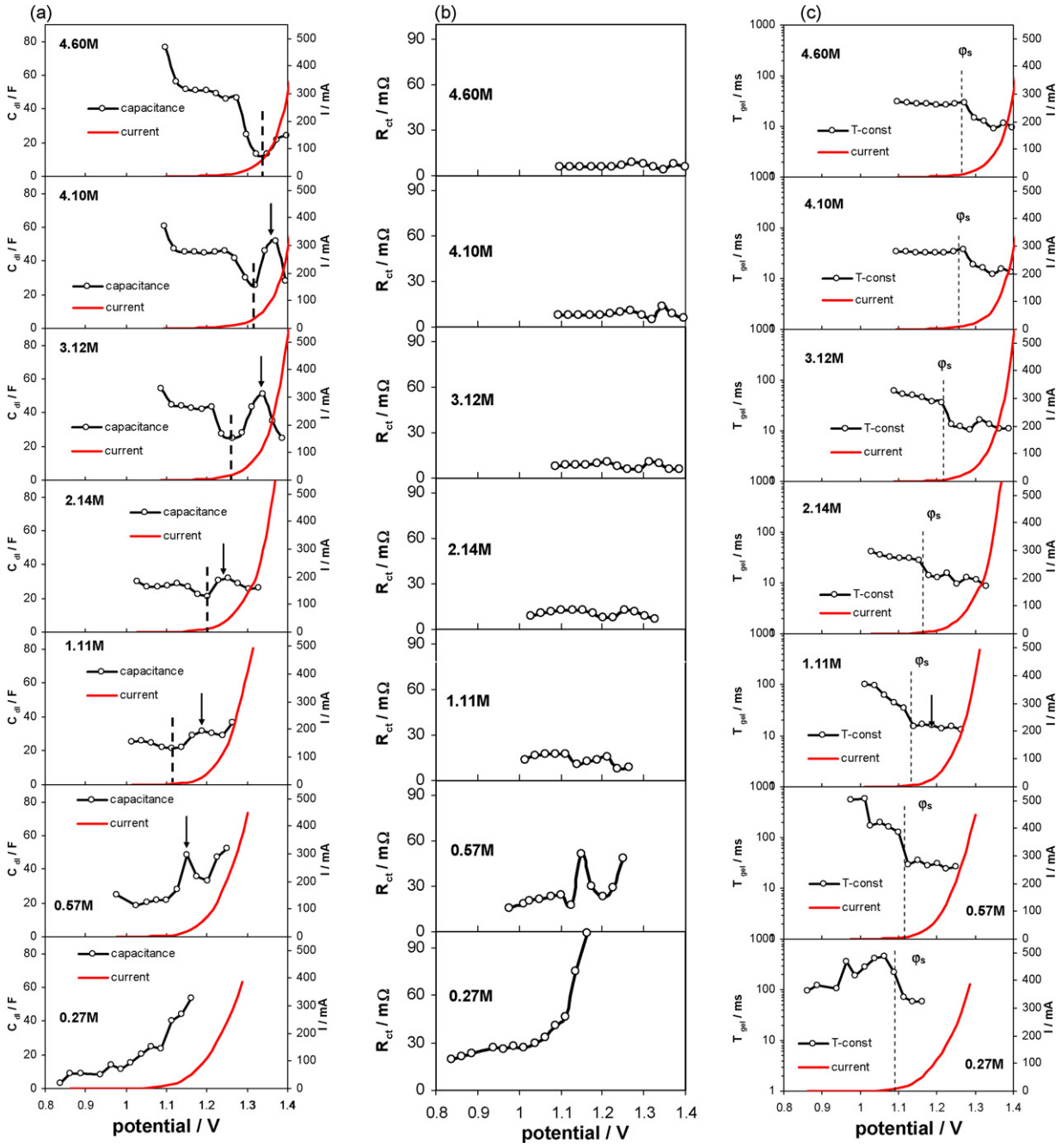

Fig. 7. Evolution of the EDL capacitance C_{dl}, the charge transfer resistance R_{ct} and the time constant of the gel part of the lead dioxide T_{gel} with the positive plate potential and $C_{H_2SO_4}$.

produces H^+ from H_2O. The drift of the PZC towards more positive potentials increasing the acid concentration is caused by the chemisorption of the acid species, which increases also with the rise of the applied potential [16]. When the acid concentration decreases, the values of PZC correspond to lower values of the oxygen evolution current. In terms of adsorption, it means that in more diluted acid when the adsorption of HSO_4^- and SO_4^{2-} is lower, the sign of the EDL charge can be changed with smaller effort by the systems, i.e. by smaller oxygen evolution current. The maximum which follows PZC in this case can be explained with adsorption/desorption of $OH^\bullet$ radicals which are electro-neutral intermediates in the oxygen evolution process [21]. At lower concentration of the acid, the maximum corresponds to lower currents of oxygen evolution, i.e. the passivation caused by the adsorption of $OH^\bullet$ radicals can be overcome easier in more diluted acid. This conclusion corresponds to the decrease of the oxygen overvoltage in the more diluted acid. In the most diluted acid, neither a minimum corresponding to PZC nor a maximum has been observed. This result can be related to some more substantial changes in the surface structure of the lead dioxide during the overcharge polarization in this acid concentration.

3.5.2. Influence of the positive plate potential on the charge transfer resistance

In the region 2–5 M, the charge transfer resistance remains rather constant both as a function of the acid concentration and of the applied electrode potential. Such result is in fair agreement with the general electrochemical kinetics theory, where the charge transfer resistance is reversely proportional to the exchange current I_0 [22]:

$$R_{ct} = \frac{RT}{I_0 F} \quad (6)$$

Decreasing the acid concentration, R_{ct} increases markedly, especially at higher polarizations.

A possible explanation can be a substantial change in the EDL structure in diluted electrolytes ($C_{H_2SO_4} < 1$ M).

3.5.3. Influence of the positive plate potential and H_2SO_4 concentration on the time constant of the gel part of the lead dioxide, T_{gel}

The analysis of T_{gel} vs. φ_+ plots confirms the above raised hypothesis about the influence of the oxygen evolution on the hydration of the lead dioxide. During the oxygen evolution H_2O molecules are decomposed to H^+ and O_2 on active centres in the gel part of the lead dioxide. This process causes local depletion of the water content in the lead dioxide and hence increases the share of the crystalline part of the lead dioxide. Thus in the region 2–5 M H_2SO_4, while the current of oxygen evolution remains low, T_{gel} is constant or decreases slowly with the increase of the potential. In the moment when φ_+ passes the φ_s-potential (this potential marks the beginning of the reaction of formation of oxygen atoms from $OH^\bullet$ radicals [11,21]) there is a sharp decrease of T_{gel} showing the dehydration of the gel–PbO_2 due to the intensive oxygen evolution. In the region 0.25–2 M H_2SO_4 at potentials closer to the open circuit potential, T_{gel} is much higher which shows that even without charge/discharge cycling the water molecules can hydrate the crystalline PbO_2 when PAM is exposed to more diluted acid [23].

3.6. Influence of the sulphuric acid concentration on the average double layer current during the pulse charge

In part I of this work we proposed the average double layer current $\langle I_{dl}\rangle$ as a simple parameter reflecting the participation of the EDL in pulse charge process, and hence a parameter related to the efficiency of the pulse charge itself [17]. $\langle I_{dl}\rangle$ can be calculated according to the following equation:

$$\langle I_{DL}\rangle = 2fC_{DL}\,\Delta\varphi_{+ON/OFF} \quad (7)$$

where $\Delta\varphi_{+ON/OFF}$ is the increase or the decrease of φ_+ during the "ON" or the "OFF" period as it is illustrated in Fig. 8. In most of the cases the shape of the pulse transients were symmetric, i.e. $\Delta\varphi_{+ON} = -\Delta\varphi_{+OFF}$ which means equality of the double layer charge and discharge current module values. We have to underline again that this approach is approximate since the values of C_{dl} measured at steady state at open circuit can differ from the dynamic values of C_{dl} during the pulse polarization (see Fig. 7a).

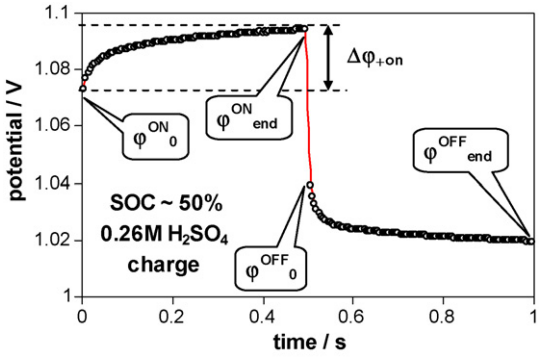

Fig. 8. Evolution of the positive plate potential during a single pulse period.

Fig. 9 presents the evolution of $\Delta\varphi_{+ON}$, C_{dl} and $\langle I_{dl}\rangle$ with the acid concentration for 0 and 50% SoC. In general the increase of the acid concentration and SoC, decreases the values of $\Delta\varphi_{+ON}$. The C_{dl} at 0% SoC in the region 3–5 M H_2SO_4 tends to zero because of the complete discharge of PAM which decreases strongly the electrochemically available surface. In more diluted acids C_{dl} remains quite high due to the capacity limitation caused by the electrolyte. Similar situation can be observed at 50% SoC—the dilution of acid combined with partial charge results in apparently constant values of C_{dl} about 30 F. The resultant

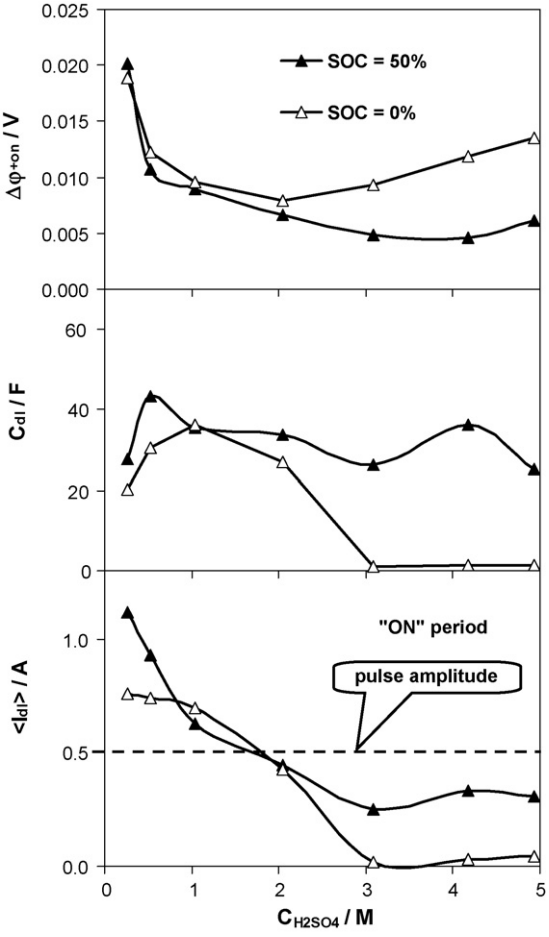

Fig. 9. Dependence of $\Delta\varphi_{+ON}$, C_{dl} and $\langle I_{dl}\rangle$ on the sulphuric acid concentration for 0 and 50% SoC.

dependence of $\langle I_{dl} \rangle$ on H_2SO_4 concentration shows that the pulse charge can be very effective in diluted acids after deeper discharges, especially of batteries with tubular design of the positive plates as well as during the pulse formation in diluted electrolytes. In these cases, we can accept that all of the current is redirected via the double layer charge and consecutive double layer self-discharge lumped with electrochemical reactions.

3.7. Influence of the sulphuric acid concentration on the average double layer current during the pulse overcharge

Using the data for the C_{dl} vs. φ_+ shown in Fig. 7a the average double layer current was calculated in the case of pulse overcharge. The obtained results for two pulse amplitudes—60 and 160 mA are presented in Fig. 10. In the region 1–5 M H_2SO_4 the calculated values of $\langle I_{dl} \rangle$ are quite close to the pulse amplitude, especially when the polarization is lower and the impedance data contain less noise. When the acid is strongly diluted ($CH_2SO_4 < 1$ M) the calculated average double layer current is much higher than the pulse amplitude. A possible explanation for such disagreement with the used approach is a non-homogeneous propagation of the current in the volume of PAM: the decrease of the acid concentration results in strong increase of the electrolyte resistance in the smallest pores of PAM. Thus the smallest pores cannot participate actively in the electrochemical processes. That is why in the Eq. (7) the value of C_{dl} should be replaced with a new value accounting only the share of PAM pores with larger diameter where the ohmic resistance is lower. The same phenomenon also limits the capacity of the positive plate in diluted electrolytes. In order to account the share of PAM participating in the discharge process we can divide the discharge capacity measured in the most diluted acid (0.37 Ah in 0.26 M H_2SO_4) to the nominal capacity of PAM typically observed in the region 3–5 M H_2SO_4 (~3 Ah)—the result shows that only 12% of the capacity is available. Let us make similar analysis with the data from Fig. 10, considering that real value of the average double layer current is equal to the amplitude of the pulse square wave. The ratio between the applied amplitude and the calculated $\langle I_{dl} \rangle$ value is about 0.13–0.14, i.e. only 13–14% of the pores surface participates in the pulse overcharge when the positive plate is polarized in 0.27 M H_2SO_4. From this coincidence it can be concluded that the dilution of the electrolyte limits the participation of the smallest pores both in the discharge and in the pulse charge process.

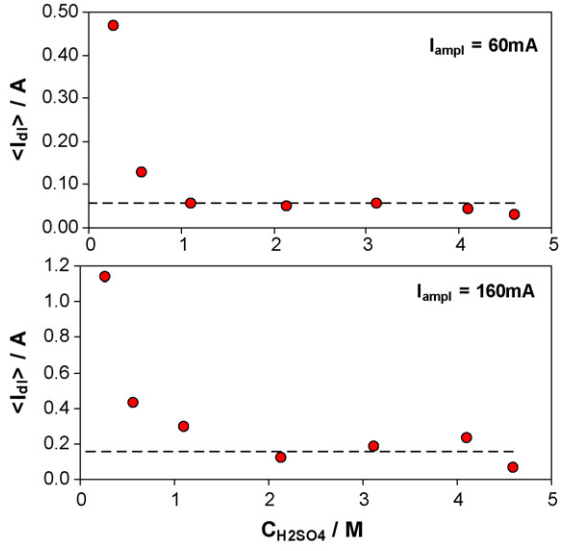

Fig. 10. Dependence of the average double layer current on the sulphuric acid concentration during pulse overcharge with amplitude 60 and 160 mA. The pulse amplitude is represented with broken line.

4. Conclusions

The obtained results show that the sulphuric acid concentration exert different effects on the processes during the exploitation of the positive plate—the dilution of the electrolyte impedes the cathodic process (the discharge) but promotes the anodic processes (the charge and the oxygen evolution). While the oxygen overvoltage decreases gradually with the decrease of the acid molarity from 5 to 0.25 M, the discharge capacity remains almost constant in the range 5–3 M and begins to decrease when the concentration becomes less than 3 M tending to zero for zero molarity of H_2SO_4. The results from the impedance measurements of the positive plate in completely charged state also can be sorted in two groups: in the region 5–2 M H_2SO_4 the ohmic resistance and the charge transfer resistance do not change substantially, but at further decrease of the acid concentration both increase markedly. Similar behaviour is observed for the time constant of the gel part of the lead dioxide, which means that below 2 M H_2SO_4, the extent of the hydration increases rapidly. Only the EDL capacitance decreases gradually with the dilution of the acid, which is almost pure adsorption effect which does not concern the hydration of the lead dioxide. The analysis of the open circuit decay transients of φ_+ confirmed that the acid dilution impedes the charge transfer during the charge/discharge process only, but not during the oxygen evolution. The previously proposed equivalent circuit model of the positive plate was successfully applied in the fitting of the impedance spectra during the potentiostatic overcharge polarization up to currents corresponding to $0.1C_{10}$ charge rates. The obtained dependence of C_{dl} on φ_+ features a minimum corresponding to the potential of the zero charge of the positive plate and a subsequent maximum corresponding to adsorption/desorption of $OH^{\bullet}$ radicals formed as intermediates during the oxygen evolution process. In partial state of charge the dilution of the electrolyte substantially increases the average double layer current and in the end of the charge, the latter becomes equal to the pulse amplitude regardless of the acid concentration.

References

[1] D.A.J. Rand, P.T. Moseley, J. Garche, C.D. Parker (Eds.), Valve-regulated Lead-acid Batteries, Elsevier, Amsterdam, 2004.
[2] F. Mattera, D. Benchetrite, D. Desmettre, J.L. Martin, E. Potteau, J. Power Sources 116 (2003) 248–256.
[3] D. Pavlov, J. Power Sources 64 (1997) 131–137.
[4] D. Pavlov, J. Power Sources 158 (2006) 964–976.
[5] D. Pavlov, V. Naidenov, S. Ruevski, J. Power Sources 161 (2006) 658–665.

[6] P. Ruetschi, J. Power Sources 116 (2002) 53.
[7] P. Ruetschi, J. Power Sources 113 (2002) 363.
[8] D. Vladikova, Z. Stoynov, G. Raikova, in: D. Vladikova, Z. Stoynov (Eds.), Portable and Emergency Energy Sources, Prof. Marin Drinov Academic Publishing House, Sofia, 2006.
[9] D. Pavlov, A. Kirchev, B. Monahov, J. Power Sources 144 (2005) 521–527.
[10] M.K. Dimitrov, J. Power Sources 90 (1990) 121–124.
[11] D. Pavlov, B. Monahov, J. Electrochem. Soc. 145 (1998) 70–77.
[12] C.H. Hsu, F. Mansfeld, Corrosion 57 (2001) 747–748.
[13] V.D. Jovic, Determination of the correct value of C_{dl} from the impedance results fitted by the commercially available software, Published on-line at http://www.gamry.com, November 2003.
[14] H. Bode, Lead-acid Batteries, John Wiley & Sons, New York, 1977, p. 75.
[15] A. Kirchev, A. Delaille, M. Perrin, E. Lemaire, F. Mattera, J. Power Sources 170 (2007) 495–512.
[16] I.G. Kiseleva, B.N. Kabanov, Dokl. Acad. Nauk SSSR 108 (1956) 864.
[17] A. Kirchev, M. Perrin, E. Lemaire, F. Karoui, F. Mattera, J. Power Sources 177 (2008) 217.
[18] B.E. Conway, J. Electrochem. Soc. 138 (1991) 1539–1548.
[19] J. Niu, B.E. Conway, W.G. Pell, J. Power Sources 135 (2004) 332–343.
[20] A.N. Frumkin, Potential of the Zero Charge, Nauka, Moscow, 1979, p. 154.
[21] D. Pavlov, B. Monahov, J. Electochem. Soc. 143 (1996) 3616.
[22] J.O'M. Bockris, A.K.N. Reddy, M. Gamboa-Aldeco, Modern Electrochemistry 2A: Fundamentals of Electrodics, 2nd ed., Kluwer Academic/Plenum Publishers, New York, 2000, p. 1056.
[23] D. Pavlov, I. Balkanov, J. Electrochem. Soc. 139 (1992) 1830–1835.